Molecular Origin of the Free Energy Dependence on the Monomer Sequence in Random Copolymer Systems

Jacek Dudowicz* and Karl F. Freed

The James Franck Institute and the Department of Chemistry, University of Chicago, Chicago, Illinois 60637

Received April 19, 1996; Revised Manuscript Received September 6, 1996[⊗]

ABSTRACT: The lattice cluster theory (LCT) is used to describe the monomer sequence dependence of the averaged free energy for an A-*co*-B random copolymer melt. This description is possible because the LCT considers local correlations (i.e., nonrandom mixing) and allows chemically different monomers to have different sizes and shapes as well as different interaction energies. In contrast to earlier theoretical approaches, the LCT treatment requires no ad hoc assumptions concerning the particular form of the sequence-dependent interaction parameters and employs no new adjustable parameters beyond those already appearing in the LCT for A/B homopolymer blends and for A-*b*-B diblock copolymer melts. The sequence-dependent contributions are extracted by comparing individual LCT diagrams for the free energy of random and diblock copolymer melts. Terms that differ for these two systems are identified as monomer sequence dependent. The sequence-dependent contributions are separated into enthalpic and entropic components. A detailed analysis of the local monomer topologies contributing to these diagrams demonstrates that the leading order sequence-dependent terms in the averaged free energy of random copolymer melts (as well as more complex mixtures) arise from diads of sequential monomers, not from triads as previously assumed.

I. Introduction

Random copolymer systems are of considerable technological importance because of the unique properties they impart to blends and other composite polymeric materials. One important feature contributing to the utility of random copolymers stems from their ability to enhance mixing of otherwise immiscible systems. For instance, polystyrene and poly(acrylonitrile) are both immiscible with poly(methyl methacrylate), but the random copolymer of styrene and acrylonitrile mixes with poly(methyl methacrylate) over a wide range of compositions. The ability of random copolymers to enhance miscibility or to produce a multiphase region with particular desired morphology has led to the development of many specialty materials and commodity polymers. The latter include polyolefin copolymers, styrene−butadiene synthetic rubbers, and blends of polycarbonate with acrylonitrile−butadiene−styrene random copolymers.[1] There is great industrial interest in these copolymers; for example, the polycarbonate blends are widely used in the automotive industry. The recent development of metallocene catalysts for polyolefin production promises to revolutionize the ability of tailoring polyolefins into thermoplastic elastomers that will replace the engineering polymers currently used in transportation. The new catalysts produce random copolymers which tend to have lower degrees of short branching in the lower molecular weight components in contrast to the older kinetically controlled copolymers which have a high degree of branching in those components. Thus, the new catalysts enable controlling the sizes of the crystalline and rubbery domains. The properties of these systems (and many other random copolymer materials) are sensitive to the details of their phase equilibria and the characteristics of the interfaces between phase-separated components.

Describing the properties of random copolymer systems presents an enormous theoretical challenge. An idealized statistical random copolymer system of polymerization index N has, in principle, 2^N different chemical components (ignoring symmetry equivalent cases). All calculated thermodynamic properties of the system must be derived from the average of the free energy over this random distribution of monomers for the two monomeric species, an average that has been termed a "quenched" average. The earliest theories[2−4] of random copolymer systems are basically applications of Flory−Huggins (FH) theory and assume the existence of a single interaction parameter χ_{ij} for each pair of different monomer species ij in the random copolymer system. Often there is no consideration of the temperature dependence of the χ_{ij}, i.e., no separation of the χ_{ij} into separate enthalpic and entropic portions. The widespread use of these earliest theories is propelled by their simplicity and by their enormous success in explaining the enhanced miscibilities observed[5] in many random copolymer containing systems, as well as in describing the general features of phase diagrams[2−4] and interfacial properties.[6] This success in describing phase diagrams is illustrated by recourse to the simplest case involving a blend of a random A-*co*-B copolymer with a homopolymer C, a system containing three different monomeric species. Assuming the blend to be incompressible, the random copolymer FH theory derives the effective interaction parameter χ_{eff} between the copolymer and the homopolymer as a weighted average of the binary interaction parameters χ_{AB}, χ_{AC}, and χ_{BC} in which χ_{AB} appears with a negative sign, thereby producing a facilitated miscibility of this system for repulsive enough AB interactions (even if the AC and BC interactions are sufficiently repulsive to ensure that blends of A with C or of B with C are immiscible mixtures). This important principle enables creating miscible blends with random copolymers or fabricating materials with particular desired morphologies and properties from other phase-separated blends.

While the Flory−Huggins (FH) random copolymer theories are immensely useful, they contain many limitations to achieving the detailed molecular understanding necessary for the control and design of mul-

[⊗] Abstract published in *Advance ACS Abstracts,* November 1, 1996.

S0024-9297(96)00587-6 CCC: $12.00

ticomponent polymer mixtures with specific properties. For example, standard FH theory does not distinguish between systems of block copolymers, random copolymers, alternating copolymers, etc., having identical monomer compositions, indicating but one severe deficiency in generally applying FH type theories to copolymers. In addition, FH theory does not adequately describe the dependence of blend properties on the monomer molecular structures and the interactions of individual constituent monomers, a problem inherent in FH theory even for homopolymer blends and perforce present for the more complicated polymer systems such as those containing random copolymers. Moreover, Flory−Huggins theory does not describe the dependence of polymer properties on the monomer sequence, resulting in identical free energies for random and diblock copolymers of the same overall composition. Recent experiments[7] for ternary mixtures of A and B homopolymers with either random A−B copolymers or purely alternating A−B copolymers exhibit different phase diagrams and therefore the existence of a sequence dependence to the system's free energy F. A similar behavior has been observed by Lohse and coworkers[8] who have studied the miscibility of atactic polypropylene with several ethylene−propylene random copolymers. All the copolymers contain 50 mol % of each monomer but vary in sequence from strictly alternating copolymers to diblocks, with a range of statistical copolymers between. The diblock is found to be the least miscible and the alternating copolymer the most. Other experiments for polybutadiene (PB) isotopic blends demonstrate[9] an inversion of the phase diagram from an upper critical solution temperature form to lower critical solution temperature diagram with an increase in the vinyl content of the protonated PB. Experimental studies of chlorinated polyethylene blends[10] likewise find a strong influence of microstructure on blend miscibility.

In order to remedy the insensivity of the earliest random copolymer theories to the monomer sequence, Balazs et al.[11] and later Cantow and Schulz[12] introduce sequence-dependent χ parameters $\chi_{ijk,lmn}$ describing interactions between a triad of sequential monomers ijk on one polymer chain and another triad sequence lmn on a second chain. This model is based on the chemical concept that the interactions between two monomers are influenced through inductive effects by the nearest neighbors directly bonded to the two interacting units. This triad model produces 16 distinct $\chi_{ijk,lmn}$ parameters,[11] each dependent on six monomers, for a random copolymer melt and therefore introduces a huge complexity into the model. This complexity stands in stark contrast to the extreme simplicity of the earlier pure FH random copolymer model which contains only pairwise monomer−monomer interaction parameter. Of the 16 possible triad−triad interaction parameters $\chi_{ijk,lmn}$, Balazs et al.[11] arbitrarily assign unique values to two of these parameters and equate all of the remaining 14 triad−triad interaction parameters to a common "average" value, leaving three new but quite ad hoc interaction parameters. Similar arbitrary assumptions are made by Cantow and Schulz.[12] In spite of these arbitrary choices in equating χ parameters, both approaches[11,12] have successfully predicted the importance of the sequence distribution on the compatability of random copolymer containing systems.

While inductive effects are known to be operative in many systems, the presence of these six-monomer interaction parameters $\chi_{ijk,lmn}$ conflicts strongly with atomistic modeling that is generally based on the use of pairwise additive potentials. Thus, a major question persits as to whether the sequence dependence of random copolymer thermodynamic properties may be understood from this customary pairwise additive viewpoint. On the other hand, one explanation for the apparent conflict between using pairwise additive and triad−triad models lies in the fact that the χ parameters are not direct measures of the microscopic interactions but are macroscopic averages of these microscopic interaction and reflect the presence of local correlations (i.e., nonrandom mixing) in the system.

Our lattice cluster theory[13] (LCT) for diblock copolymers provides simple insight into the existence and origins of the sequence-dependent free energy contributions for random copolymer systems. The theory has already predicted[13,14] a nonnegligible contribution j/N (where N is the polymerization index and j is rather large) to the diblock copolymer free energy F from the presence of a single A−B junction bond between the two blocks. Since an average random copolymer chain has a large number of such A−B "junctions", the j/N junction dependent contribution to F (and hence to χ_{eff}) for the block copolymer melt translates into a sequence dependence of F for the random copolymer system. Thus, let the number of A−B junctions in a single random copolymer chain be cN where $c < 1$. This simple analysis yields a "junction" correction to the random copolymer melt F as $(j/N)(cN)$, which is of order N^0 as opposed to the j/N junction contribution for diblock copolymers (with j rather large). In addition, this argument suggests that the leading sequence-dependent contributions to F appear from the correlations between bonded monomer diads on a single chain.

As mentioned above, the FH random copolymer model does not distinguish between diblock, random, graft, etc., copolymers (at fixed monomer composition). The approach of Balazs et al.[11] with three arbitrarily chosen interaction parameters does introduce a physically realistic sequence dependence to F, but this is accomplished only at the expense of introducing at least three ad hoc new empirical parameters for each pair of monomer species. Furthermore, if the theory is to be used for understanding and predicting the temperature dependence of thermodynamic properties, then the division of these triad−triad interaction parameters into entropic and enthalpic portions would produce six new parameters whose relation to monomer structures and interactions is completely unknown. Moreover, the incompressible FH formulation is incapable of describing the important pressure dependence of thermodynamic properties. A theory which treats the polymer liquids as compressible systems is required for this purpose.

The above discussion provides ample motivation of the need for understanding at a more microscopic level the origins of sequence-dependent thermodynamic properties in copolymer systems, as well as for providing a systematic theoretical description of this sequence dependence using a far smaller number of adjustable parameters than those in the Balazs et al.[11] and Cantow and Schulz[12] approaches. Such a theory must relate the sequence-dependent properties to the detailed chemical structures of the monomers and to their mutual interactions.

The above questions can be addressed by the LCT which has been developed[13,15−19] to describe a rich variety of polymeric liquids. The lattice cluster theory is based on the generalized lattice model that endows the monomers with specific structures by allowing them to occupy several lattice sites with specified connectivity,

a generalization elevating the lattice model description of polymer systems to a new molecular based level.[19] The introduction of monomer molecular structures into the theoretical treatment is an essential ingredient in providing a molecular explanation for the existence of an entropic contribution to the effective interaction parameter χ_{eff} and for explaining the general observations of a composition, temperature, pressure, and molecular weight dependence of χ_{eff}. These descriptions, in turn, are only possible because the LCT considers the short-range correlations (i.e., nonrandom mixing phenomena) that are present in polymer systems as a result of the packing constraints and the different microscopic monomer-monomer interaction energies $\{\epsilon_{\alpha\beta}\}$, a feature possible only by virtue of our far superior solutions to the lattice model than those presented by FH theory. The inclusion of contributions from local correlations makes the analytical expressions for F lengthy and algebraically complicated. However, these expressions apply to all compositions, molecular weights, (higher) temperatures, and monomer structures. Moreover, the noncombinatorial portion of F is in the simple form of polynomials in the polymer volume fractions, a form easily used for computing all other properties, including the phase diagrams. The benefits of analytical tractability and of the generalized lattice model currently far outweigh the inherent limitations of any lattice model. The LCT is also ideally suited to describing the sequence dependence in random copolymers because this sequence dependence is a consequence of those local correlations that are included in the LCT contributions to the free energy F of random copolymer systems.

The germ of the methods necessary for extending LCT to random copolymers is already present in our recent papers.[13,16,18] The description of the far more complicated random copolymer system requires considering the LCT diagrams for all possible local monomer sequences, with a subsequent average over a quenched random distribution of all monomer sequences. This averaging seriously compounds the difficulty of the otherwise lengthy and complicated LCT computations for homopolymers and for diblock copolymers. While the random copolymer system should actually be treated as a multicomponent system with roughly 2^N chemically different species, this complexity is avoided at the outset by using the customary procedure of treating the random copolymer as a one-component system[2−4,11,12] and by evaluating the quenched average of the free energy.

Our primary goal is to determine the nature of the leading order sequence-dependent contributions to F. This goal includes specifying which monomer sequences provide the sequence-dependent contributions, as well as determining whether the contributions are purely energetic in origin or whether they also have an entropic (temperature independent) component. The specification of the molecular configurations (on the monomer and submonomer scales) producing the leading sequence-dependent portions of F is also of interest since a knowledge of these configurations can be helpful in guiding the modification and control of the sequence dependence and hence the properties of random copolymer systems.

Overcoming the serious technical difficulties related to the calculation of quenched averages of F is still not sufficient to extract the sequence-dependent terms (and the particular configurations generating them) from the lengthy LCT expressions for F. Therefore, we compare the LCT free energies F_{random} and F_{diblock} for random and diblock copolymer melts, respectively, by considering individual terms corresponding to the same LCT diagrams contributing to F_{random} and F_{diblock} and by analyzing only terms that are different for these two systems. The present paper illustrates the general structure of the leading contributions for a random copolymer melt, but the same results apply to various mixtures of AB random copolymers with A, B, or C homopolymers, A_xB_{1-x}/A_yB_{1-y} random copolymer mixtures, etc. A complete formulation of the new theory as well as the computations of phase diagrams will be published elsewhere.[20] Our goal here is to extract the nature and molecular origins of the leading sequence-dependent contributions to the free energy F and to explain the local chain configurations producing these contributions. It should be emphasized that the final LCT theory for AB random copolymer melts has *no new adjustable parameters* beyond those already appearing in the LCT theory for A/B homopolymer blends or A-*b*-B diblock copolymer melts. The three microscopic attractive (pairwise additive) interaction energies ϵ_{AA}, ϵ_{BB}, and ϵ_{AB} are common parameters to the LCT for all types of polymer systems containing monomers of species A and B.

Section II briefly describes the generalized lattice model for an A−B random copolymer melt and introduces the necessary notation. The basic features of the LCT are sketched in section III, with special emphasis placed on the diagrammatic representation of the free energy F and the quenched random average. Section IV analyze examples of each category of LCT diagrams that contribute to the monomer sequence dependence of F. The Appendixes provide some computational details illustrating the relation of this dependence to the monomer structures and their different interactions $\{\epsilon_{\alpha\beta}\}$.

II. Model and Notation

The theory is developed here for the limit of a completely random copolymer melt whose composition is specified by the average numbers of monomers in the system for each of the two species. With some additional difficulty, the formulation may be extended to copolymers with kinetically controlled monomer sequences. A random copolymer melt is represented here as a set of n monodisperse chains placed on a regular array of N_l lattice sites and coordination number z. A single chain consists, on average, of n_A monomers of species A and n_B monomers of species B that are distributed randomly along the chain backbone. In a chain with average composition these monomers are joined by $n_A + n_B - 1$ backbone bonds, and there are $n_A(n_A-1)/(n_A + n_B)$ connecting bonds between successive AA monomers, $n_B(n_B-1)/(n_A + n_B)$ connecting bonds between BB pairs, and $2n_An_B/(n_A + n_B)$ junction bonds between AB or BA monomers, producing a total of $n_A + n_B - 1$ connecting bonds.

We consider the composition of the many copolymer chain system to be determined by the relative fractions of A and B monomers initially present in the reaction system. However, the chains are taken to be monodisperse, for simplicity. In principle, each possible sequence for the random copolymer is a distinct chemical species and should be treated as a separate entity. Thus, a chain with N total monomers implies the presence of roughly 2^N different chemical species. Hence, a rather unwieldy analysis is necessary to describe such a multicomponent mixture. Instead, we follow the customary procedure of treating the random copolymer melt as a one-component system with certain average values of n_A and n_B monomers per chain. The

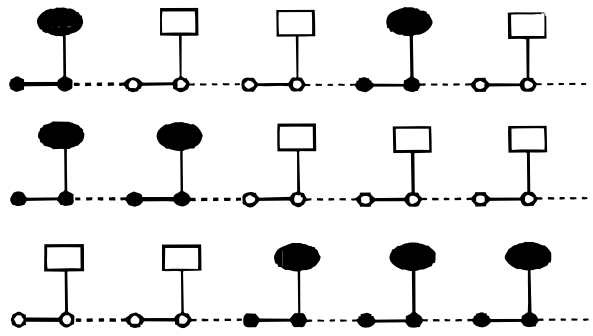

Figure 1. Vinyl monomer model for random and diblock copolymer chains with $n_A = 3$ and $n_B = 2$ monomers of species A and B, respectively. The random copolymer chain is at the top of the figure, while the two bottom patterns depict the diblock copolymer chain with the two possible block sequences. Submonomer units (e.g., united atom groups) along the chain backbone are denoted by circles, while the side groups are represented simply as squares and circles. Backbone bonds within monomers are designated by solid lines, and the connecting bonds are represented by dashed lines.

general theory, however, must introduce a complete statistical average (called a quenched average) of the free energy over all these roughly 2^N sequences for all chains in the random copolymer melt. This need for applying a quenched average leads to considerable technical difficulties, but, as discussed later, our approach of treating the system as one component and of computing the quenched average free energy is sufficient to understand and elucidate the molecular origins of sequence-dependent effective interactions in random copolymer systems.

The chain occupancy index M is defined as $M = n_A s_A + n_B s_B$, where s_α designates the number of lattice sites occupied by a single monomer α. The values of s_A and s_B are chosen to reflect the relative monomer sizes, while the monomer architecture is designed to mimic the monomer structure in, for example, united atom models.

To make the general theory applicable to the majority of experimental systems, individual monomers of both species are assigned vinyl structures that spread over several lattice sites. Figure 1 depicts one example of such a random copolymer chain for a particular monomer sequence. Small circles refer to individual submonomer units that occupy single lattice sites. Each monomer contains two united atom groups that form a portion of the chain backbone and that lie on separate lattice sites. Each monomer is also taken to have single side groups occupying at least one lattice site. The side groups are schematically represented in Figure 1 by circles and squares, but the side groups may have particular geometries as illustrated, for example, in Figure 1 of ref 21. (Models with monomers other than vinyl are readily considered with minor modifications to the general theory.) The bottom two portions of Figure 1 depict two different models for the corresponding diblock copolymer chain. The diblock models are used in comparisons between random and diblock copolymer systems to aid in understanding the computed sequence dependence. The presence of explicit monomer structures makes the diblock chains with sequences $(A)_{n_A}-(B)_{n_B}$ and $(B)_{n_B}-(A)_{n_A}$ inequivalent. These two structures in Figure 1 are not mirror images of each other.

The existence of nonzero melt compressibility (i.e., of a nontrivial equation of state) implies the presence in the system of excess free volume, which is modeled by n_v empty sites with a volume fraction of $\phi_v \equiv n_v/N_l = 1 - nM/N_l = 1 - \phi$. The excess free volume fraction ϕ_v is determined for given pressure P and temperature T from the equation of state. The lattice is assumed to be a three-dimensional ($d = 3$) cubic lattice with $z = 2d = 6$.

Excluded volume constraints prohibit any two submonomer units from lying at the same lattice site and naturally represent the short-range repulsive interactions. Longer range attractions are introduced by ascribing the attractive microscopic van der Waals energy $\epsilon_{\alpha\beta}^{i,j}$ to nearest neighbor (on the lattice) portions i and j of the monomers α and β (with α and β chosen from the A and B monomers). All the s_α portions of a given monomer are taken as energetically equivalent units. Thus, these s_α subunits interact with any of the s_β portions of a monomer β with the same average energy $\epsilon_{\alpha\beta}$. Hence, the model of a random A/B copolymer melt contains three independent microscopic energetic parameters ϵ_{AA}, ϵ_{BB}, and ϵ_{AB}. The theory may, in principle, ascribe different interactions to each of the chemically different subgroups of the individual monomers, but we retain the minimal three-interaction model to avoid the proliferation of adjustable parameters until experimental data cannot be explained by employing only the three $\epsilon_{\alpha\beta}$. The same three interaction energies also apply to the treatment of binary A/B homopolymer blends and A-*b*-B diblock copolymer melts. The presence of three microscopic interaction energies leads to important energetic consequences of "compressibility" that supplement the usual free-volume-type "equation of state effects" and that are absent in one-parameter FH type theories.

III. Basic Features of the Lattice Cluster Theory

The generalized lattice model of polymer systems is solved[16] by using cluster expansion methods, which explicitly consider short-range correlations that are present in polymer systems as a result of packing constraints and the different interactions $\{\epsilon_{\alpha\beta}\}$. The introduction of these local correlations into the theory is a crucial ingredient in enabling the theory to describe the sequence and monomer structure dependence of thermodynamic properties and, for instance, the different thermodynamic behaviors of random and diblock copolymers. The extension of the classic Flory−Huggins (FH) theory to random copolymers neglects all these correlations and therefore does not distinguish between random copolymers, diblock copolymers, alternating copolymers, etc. Nevertheless, the random copolymer version of a compressible generalization of FH theory emerges in the LCT as the zeroth-order approximation.

The Helmholtz free energy F of the system is computed as a perturbative expansion about the FH free energy F^{FH}. The LCT free energy F can be written[16] in simple symbolic form as

$$\frac{F}{N_l k_B T} - \frac{F^{FH}}{N_l k_B T} = \text{corrections} = \frac{1}{N_l}\sum_{b,l} \text{cumulant diagrams} = \sum_{b,l}\sum_{i=1} C_i(b,l) \quad (3.1)$$

where the corrections to the compressible system generalization of the Flory−Huggins approximation F^{FH} in eq 3.1 are conveniently represented in terms of cumulant contributions $C_i(b,l)$ from the cumulant cluster diagrams $D_i(b,l)$ with b bonds and l interaction lines. The sequential index i labels the diagrams with the same b and l.

Some terminology associated with the diagrams can be explained with recourse to Figures 2 and 3 which

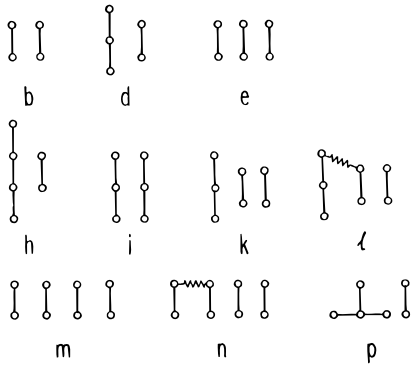

Figure 2. Athermal limit packing entropy ($S^{\infty}_{\rm ncom}$) diagrams describing the corrections to the Flory−Huggins packing entropy of a random copolymer melt through order z^{-2}. Circles represent monomer portions lying at single lattice sites, and solid lines designate correlating bonds. Wiggly lines in diagrams l and n indicate bonds that occur nonsequentially on a single chain. The figure depicts only the diagrams contributing at least bilinearly in the volume fraction ϕ to $S^{\infty}_{\rm ncom}$, i.e., describing correlations between bonds located at minimum on two chains. The structure of the diagrams remains the same for all liquid state polymer systems, including homopolymer and copolymer melts or multicomponent blends.

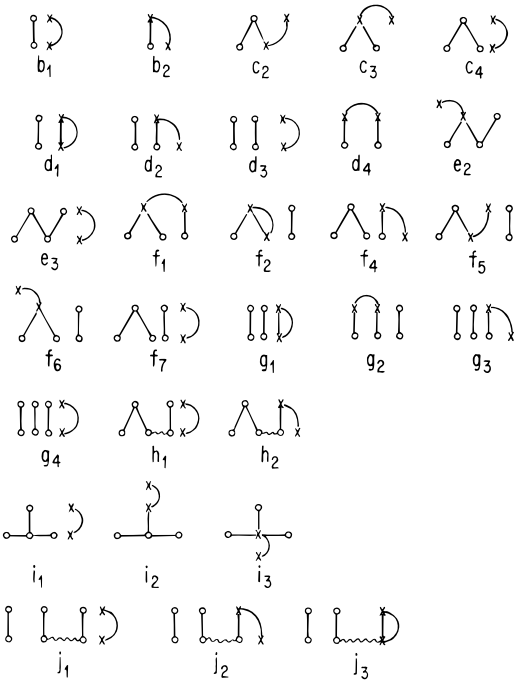

Figure 3. First-order energy diagrams describing the corrections to the averaged FH Helmholtz free energy of a random copolymer melt through order z^{-2}. Crosses and circles are used to distinguish between interacting and noninteracting monomer portions, respectively. The curved lines denote interactions of nearest-neighbor submonomer units, while straight lines depict the correlating bonds. As in Figure 2, we present only the diagrams contributing beyond the linear power of ϕ to the averaged free energy $\bar{F}$. The structure of the diagrams is identical for different polymer systems, such as homopolymer and copolymer melts or multicomponent blends.

are discussed more fully below. The circles in Figure 2 indicate submonomer portions lying on individual lattice sites (as in Figure 1), while the lines joining the circles represent the actual chemical bonds connecting these units. The bonds appearing in Figure 2 are called "correlating" bonds because their contributions to the *corrections* in eq 3.1 arise from the local packing induced correlations between the sets of bonds indicated in the diagrams. The two bonds in diagram b of Figure 2 lie on different chains, while the leftmost pair of bonds in diagram d are sequential bonds on a single chain. Nonsequential bonds of the same chain are connected in a diagram by a wiggly line as in diagrams l and n of Figure 2. The diagrams in Figure 2 contain up to four correlating bonds, but the diagrams in Figure 3 may have curved "interaction lines" in addition to the correlating bonds. These curved lines indicate the presence of the attractive van der Waals interaction $\epsilon_{\alpha\beta}$ between the nearest-neighbor submonomer portions of species α and β. The interacting submonomer units are denoted in a diagram by crosses even if they are also linked by a correlating bond.

The cumulant diagrams $D_i(b,l)$ of eq 3.1 are simple algebraic combinations of the individual LCT diagrams that are naturally formed when taking the logarithm of the partition function.[16] The cumulants ensure the extraction from the diagrams in Figures 2 and 3, etc. of the proper portions that in the thermodynamic limit ($n \rightarrow \infty$, $N_l \rightarrow \infty$, but $\phi \equiv nM/N_l = \text{const}$) yield only extensive contributions, proportional to the number of lattice sites N_l. Each of these extensive terms is also finite in the long chain limit ($M \rightarrow \infty$). Our discussion of the origin of sequence-dependent effective interactions does not require the detailed description of the cumulant diagrams,[16] so the discussion below of the complete sequence dependence is deduced solely from the extensive portions of the individual diagrams in Figures 2, 3, etc. Diagrams with $l = 0$ and $b \neq 0$ in Figure 2 provide the noncombinatorial athermal limit entropy $S^{\infty}_{\rm ncom}$, while diagrams with $b = 0$ and $l \neq 0$ (not shown) are monomer structure independent energy diagrams having only interaction lines. Because the leading energy diagram (with $b = 0$ and $l = 1$) arises from the interaction between two uncorrelated monomer subunits, it contributes to the random copolymer compressible FH free energy $F^{\rm FH}$ and is excluded from the sums in eq 3.1.

As noted above, the free energy expression in eq 3.1 must be averaged over all possible sequences of A and B monomers in all chains of the system. This quenched random average, therefore, implies that the set of b correlating polymer bonds in each diagram of Figures 2 and 3 must be chosen in all possible ways from bonds interior to monomers A and/or B (lying on either the backbone or side groups) and from the connecting bonds between monomers. (See Figure 1 for the identification of interior and connecting bonds.) The sequence-averaged free energy must subsequently be averaged over all possible values of $n_{\rm A}$ and $n_{\rm B}$, subject to the constraints on the average numbers of monomers in the whole many-chain system and the (convenient but not necessary) constraint of monodisperse chains. For simplicity of presenting the basic physical concepts and the results, the computations below consider the more difficult and fundamental average of the free energy only over all possible sequences in chains having exactly $n_{\rm A}$ and $n_{\rm B}$ monomers of the two species. The second average over $n_{\rm A}$ and $n_{\rm B}$ is quite straightforward and does not change the basic structure of the final results.

The l interacting lines in Figure 3 terminate on interacting monomer subunits, which are likewise chosen in all possible ways from all the submonomer units in the system. In particular, interaction lines may even connect monomer portions that are linked by correlating bonds in the diagram. In other words, we must also include diagrams with the interaction line(s) between two bonded (i.e., correlated) monomer units (e.g., diagrams d_1, f_2, or g_1 of Figure 3). The presence of these diagrams in eq 3.1 follows naturally in the derivation of the lattice cluster theory. Ignoring these diagrams violates, for example, Madden's theorem[22] which notes

that excess thermodynamic properties of binary blends depend in the incompressible limit only on a single microscopic exchange energy $\epsilon = \epsilon_{AA} + \epsilon_{BB} - 2\epsilon_{AB}$. The inclusion of these diagrams in the LCT contrasts with the simple FH treatment of polymers as uncorrelated systems. Within simple FH-like theories, the inclusion of interactions between bonded nearest-neighbor monomers of the same chain merely shifts the zero of energy without affecting the system's thermodynamics.

Specifying the numbers of bonds and interacting lines alone does not fully describe a diagram. A complete description requires information concerning the location of the interaction lines with respect to the correlating bonds and information on whether the correlating bonds belong to one chain or to many. Thus, when correlating bonds lie on a common chain, the diagrams distinguish sequential and nonsequential sets of correlating bonds. Figure 2 depicts the relevant athermal limit entropy (S^{∞}_{ncom}) diagrams with up to $b = 4$ correlating bonds. Wiggly lines in diagrams *l* and *n* indicate the nonsequential occurence of bonds in a single chain. Only diagrams contributing to S^{∞}_{ncom} beyond linear powers of ϕ are presented in the figure.[23] Diagrams with one interaction line are called first-order energy diagrams. Figure 3 illustrates all the first-order energy diagrams that contribute (at least bilinearly in the polymer volume fraction) to the Helmholtz free energy (3.1) through order z^{-2} (beyond the compressible FH approximation, i.e., beyond the diagram with $b = 0$ and $l = 1$). Only diagrams with $b \leq 3$ are required to this order. Crosses and circles in the diagrams of Figure 3 accentuate the difference between interacting and noninteracting monomer segments, respectively. The ends of the interaction lines may be disconnected from (see, for instance, diagrams b_1, c_4, d_3, or f_7 of Figure 3) or connected to correlating bonds (at one or both ends). Diagrams b_2, c_2, or d_2 of Figure 3 provide examples of singly connected first-order energy diagrams, while diagrams d_1, d_4, f_1, or f_2 are called doubly connected because both ends of the interaction line join monomer portions of either one or two chains. The next section describes those leading athermal limit entropy and first-order energy diagrams (from Figures 2 and 3, respectively) whose contributions produce a monomer sequence dependence to the free energy for a random copolymer melt. A comparison with the corresponding values from the same diagrams for diblock copolymer melts elucidates more fully the nature of the sequence dependence. Clearly, diagrams producing the same expressions for diblock and random copolymer melts are considered as sequence independent. This criterion represents, however, a necessary but not sufficient condition for the presence of sequence dependence.

IV. Monomer Sequence Dependence of Free Energy for Random Copolymer Melts

According to eq 3.1, the lattice cluster theory provides the Helmholtz free energy as a sum of the FH zeroth-order free energy F^{FH} and correlation-induced corrections which are conveniently written in a diagrammatic representation, reminescent of Mayer's cluster expansion for real gases. The average of the compressible system generalization of the FH free energy F^{FH} over all random copolymer sequences in the melt is given by

$$\frac{\bar{F}^{FH}}{N_l k_B T} = -\frac{\bar{S}_{com}}{N_l k_B} + \frac{z}{2}\phi^2[\epsilon_{AA} m_A{}^2 + \epsilon_{BB} m_B{}^2 + 2\epsilon_{AB} m_A m_B] \quad (4.1)$$

where $\bar{S}_{com}$ denotes the combinatorial entropy, $m_\alpha = n_\alpha s_\alpha/(n_A s_A + n_B s_B)$ is the site occupancy fraction for monomer portions of species α, $\phi = nM/N_l$ is the polymer volume fraction, and the nearest-neighbor attractive van der Waals energies $\{\epsilon_{\alpha\beta}\}$ are expressed in units of $k_B T$. When $s_A = s_B = 1$, eq 4.1 recovers the compressible system generalization of the well-known random copolymer FH expression derived by Kambour et al.[3] and ten Brinke et al.[4] While the FH energy term in eq 4.1 is identical for random and diblock A/B copolymers with the same composition $f = n_A/(n_A + n_B)$, the combinatorial entropy $\bar{S}_{com}$ differs for these two systems by an extra term arising from the average over the monomer distribution in a random copolymer chain. This monomer sequence dependent contribution is, however, linear in the volume fraction ϕ and, therefore, is ignored here. Our interest lies in probing only those terms in eq 3.1 that appear with higher than linear powers of ϕ, i.e., that contribute to the second derivative $\partial^2\bar{F}/\partial\phi^2$ of the averaged free energy $\bar{F}$ and, hence, to the spinodals.

Monte Carlo computations have been useful in assessing the accuracy of various truncations of the LCT expansion. The series in eq 3.1 has been tested[15] for an incompressible polymer−solvent system (or equivalently a compressible polymer melt) by comparison with Monte Carlo simulations[15] of the identical lattice model for this mixture. Terms through orders $(1/z)^2$ and $(\epsilon/k_B T)^2$ are found to be the most important for a one-component polymer melt and to be sufficient in representing the LCT free energy F and its first and second composition derivatives. Additional tests for polymer blends or copolymer melts would be desirable, but the lack of Monte Carlo data for these systems currently precludes these useful tests.

The correction terms through orders $(1/z)^2$ and $(\epsilon_{\alpha\beta}/k_B T)^2$ correspond to diagrams where the sum of b correlating bonds and l interaction lines does not exceed four ($b + l \leq 4$) and l is not greater than two ($l \leq 2$). Among the diagrams that satisfy these conditions, only diagrams consisting exclusively of interactions lines (called extended mean field diagrams) cannot a priori contribute to the monomer sequence dependence of $\bar{F}$. The extended FH mean field diagrams have no correlating bonds ($b = 0$) and, therefore, are insensitive to the monomer sequence. Our study for the monomer sequence dependence of $\bar{F}$ focuses on the analysis of the athermal limit entropy diagrams in Figure 2 and of the first-order energy diagrams in Figure 3, which become dominant at higher temperatures. Performing the quenched random average for these diagrams "merely" requires allowing each of the correlating and interacting subunits in the diagram to range in all possible ways over A and B monomer backbone and side group portions. For example, diagram *b* of Figure 2 can have both bonds lying within monomers of species A or B, one in A and one in B, both as connecting bonds (either A−A, B−B, or A−B), etc. A similar type of analysis can readily be applied to the second-order energy diagrams. However, their contribution to the LCT energy of mixing and the coexistence curves becomes less important[15] for typical melt densities corresponding to $\phi \geq 0.8$. Hence, these more numerous and complicated second-order contributions are not analyzed here.

Each of the diagrams in Figures 2 and 3 exhibits an explicit dependence on the monomer structures, i.e., on their sizes, shapes, and bonding patterns. Many diagrams have contributions from portions of a single chain that involve more than one monomer, but it is not obvious at all judging from the values of individual diagrams whether these contributions constitute a sequence dependence to $\bar{F}$. Thus, we use the following

method to separate and determine the sequence-dependent terms. The value C_i^{random} of a given diagram i for a random copolymer melt is compared with the value C_i^{diblock} of the same diagram i for the corresponding diblock copolymer system, and the diagrams producing a nonzero $\Delta_i = C_i^{\text{random}} - C_i^{\text{diblock}}$ are identified as the sequence-dependent contribution to $\bar{F}$. The next step is to identify the particular configurations that contribute to a nonvanishing Δ_i. For the purpose of this comparison, the model for the diblock copolymer chain is chosen as an "average" of the two possible diblock structures of Figure 1. This average is chosen because the presence of vinyl monomer structures introduces a slight asymmetry to the diblocks corresponding to the distinct chain sequences $(A)_{n_A} - (B)_{n_B}$ and $(B)_{n_B} - (A)_{n_A}$ shown in the two bottom portions of Figure 1. The "average" over the two diblock sequences removes this chemically realistic, but mathematically inconvenient, asymmetry, as explained in Appendix B.

A detailed analysis of the athermal limit entropy diagrams $D_i(b,l=0)$ emerging from the individual diagrams of Figure 2 (for $b \leq 4$) leads to the conclusion that only diagrams h and l of this figure produce contributions C_i that are monomer sequence dependent. Both diagrams delineate sets of four correlating bonds located on two different chains in such a way that three correlating bonds belong to the first chain, while the fourth one pertains to the second chain. These three bonds may, in turn, occur sequentially in a chain as is illustrated in diagram h or nonconsecutively as shown in diagram l. Contributions from individual diagrams with distant nonsequential bonds on a single chain diverge in the long chain limit ($M \rightarrow \infty$), but this singularity cancels identically upon combining these diverging terms with those that arise from diagrams with similar groups of bonds lying on separate chains. The latter cancellation is a direct consequence of the Flory theorem[24] that notes the physical indistinguishability between distant units along the same chain and those lying on different chains. This Flory theorem cancellation therefore explains why diagram l is grouped together with diagram k of Figure 2 in the computation of the LCT free energy.

The contributions C_h and C_{l+k} from the cumulant diagrams $D_h(b=\{1;3\},l=0)$ and $D_{l+k}(b=\{1,2;1\},l=0)$ can be expressed in the simple general form as

$$C_i^{\text{random}} = X_i + Y_i^{(A)}[n_A - n_A/(n_A + n_B)] + Y_i^{(B)}[n_B - n_B/(n_A + n_B)], \quad i = \text{h and l + k} \quad (4.2)$$

for random copolymers with n_A and n_B monomers for species A and B and as

$$C_i^{\text{diblock}} = X_i + Y_i^{(A)}(n_A - {}^1/_2) + Y_i^{(B)}(n_B - {}^1/_2), \quad i = \text{h and l + k} \quad (4.3)$$

for the diblock copolymers also with n_A and n_B monomers of species A and B. (The averaging over the two diblock structures in Figure 1 leads to the appearance of the $^1/_2$ in eq 4.3 and in some other diblock diagram values below). Both X_i and $Y_i^{(\alpha)}$ in eqs 4.2 and 4.3 are functions of the polymer volume fraction $\phi = 1 - \phi_v$, the lattice coordination number z, and the chain occupancy index $M = n_A s_A + n_B s_B$, and both depend on the monomer structures. This monomer structure dependence enters into C_i through a set of geometrical coefficients that describe the number of ways for selecting a given configuration of bonds (depicted by a diagram) from all the bonds in a single chain and through the monomer's site occupancy indices s_A and s_B. Explicit expressions for X_h, X_{l+k}, $Y_h^{(\alpha)}$, and $Y_{l+k}^{(\alpha)}$ (α = A and B) are given in Appendix A, but are not required here.

The X_i contributions in eqs 4.2 and 4.3 are sequence independent. However, a portion of the contribution involving the $Y_i^{(\alpha)}$ differs between the diblock and random copolymers, thereby providing a sequence-dependent contribution to the total sequence-averaged free energy. The quantities $Y_i^{(A)}$ and $Y_i^{(B)}$ of eqs 4.2 and 4.3 contribute to the overall averaged free energy in order $1/M$, while the leading terms of the X_i's are of order M^0. Hence, both the $Y_i^{(A)}[n_A/(n_A + n_B)]$ and $Y_i^{(B)}[n_B/(n_A + n_B)]$ terms are formally of the same order in molecular weights as the combinatorial entropy term $(1/M)\ln \phi$. Thus, these terms are retained as possibly being important in determining, for instance, the phase behavior for random copolymer melts, blends, etc. Because the contributions C_i^{random} and C_i^{diblock} from eqs 4.2 and 4.3 coincide with one another when $f = {}^1/_2$, i.e., when $n_A = n_B$, the monomer sequence dependence of the athermal packing entropy is limited to random copolymer melts with different average numbers of monomers A and B in a single chain. An essential condition for the presence of this sequence dependence is a difference in molecular structures for monomers of species A and B. Otherwise, the terms $Y_i^{(A)}$ and $Y_i^{(B)}$ become identical, producing $C_i^{\text{random}} = C_i^{\text{diblock}}$ even if $n_A \neq n_B$ (see Appendix A). The difference in the molecular structures of monomers A and B begins to produce entropic manifestations of sequence dependence for vinyl monomer structures (see Figure 1) when the diagram contains three consecutive correlating bonds on a single chain (e.g., diagrams h and l in Figure 2). Two of these three correlating bonds belong to either a single A or B monomer, while the third one is the bond connecting this monomer with the monomer to its right in the top chain of Figure 1. The leading order sequence-dependent contribution thus emerges within the LCT from a pair of consecutive monomers rather than from a triad of monomers on a chain as assumed in the theories of Balazs et al.[11] and Cantow and Schulz.[12]

While the difference in the monomer structures of species A and B leads to the monomer sequence dependence of the athermal limit packing entropy, the presence in a random copolymer melt of the three different interaction energies ϵ_{AA}, ϵ_{BB}, and ϵ_{AB} already produces a sequence dependence to the internal energy. All the first-order energy diagrams of Figure 3 with the interaction line singly connected to the correlating bond (i.e., diagrams b_2, c_2, c_3, d_2, e_2, $f_4 - f_6$, ...) contribute to the monomer sequence dependence of F in order $1/M$. The values for this class of diagrams are summarized, using a similar notation as employed in eqs 4.2 and 4.3, by

$$C_i^{\text{random}} - C_i^{\text{diblock}} = \bar{\epsilon}_A Y_i^{(A)}[n_A/(n_A + n_B) - {}^1/_2] + \bar{\epsilon}_B Y_i^{(B)}[n_B/(n_A + n_B) - {}^1/_2] \quad (4.4)$$

where the average energy variables are $\bar{\epsilon}_A = \epsilon_{AA} m_A + \epsilon_{AB} m_B$, $\bar{\epsilon}_B = \epsilon_{BB} m_B + \epsilon_{AB} m_A$, with $m_\alpha = n_\alpha s_\alpha / M$. The $Y_i^{(A)}$ differs from $Y_i^{(B)}$ only for diagram e_2 of Figure 3. In analogy to the $Y_i^{(A)}$ and $Y_i^{(B)}$ from eqs 4.2 and 4.3 for the entropy diagrams, all the $Y_i^{(A)}$ and $Y_i^{(B)}$ ($i = b_2, c_2, c_3, d_2, e_2, ...$) of eq 4.4 are functions of M, z, and ϕ.

Moreover, the difference $C_i^{\text{random}} - C_i^{\text{diblock}}$ likewise vanishes for symmetric random copolymer chains with $f = {}^1/_2$, i.e., with $n_A = n_B$. Appendix B describes some technical aspects of deriving eq 4.4. Nonzero values of $C_i^{\text{random}} - C_i^{\text{diblock}}$ in eq 4.4 appear only when certain correlating bonds of the diagram belong to the $(n_A + n_B - 1)$ connecting bonds between sequential monomers in the chain. While the random and diblock chains have the same number (n_A+n_B-1) of connecting bonds, their partitions between AA, BB, and AB connecting bonds are clearly very different. The diblock copolymer has only one AB connecting bond, while the random copolymer chain generally contains many. As a consequence, the random copolymer contributions $Y_i^{(A)}[n_A/(n_A + n_B)]$ and $Y_i^{(B)}[n_B/(n_A + n_B)]$ of eq 4.4 depart from the terms $(1/2)Y_i^{(A)}$ and $(1/2)Y_i^{(B)}$ that represent a diblock copolymer system (with the average of the two bottom structures in Figure 1). (More detailed explanations are given in Appendix B.)

First-order ($l = 1$) energy diagrams with two or three correlating bonds still exhibit a $1/M$ monomer sequence dependence provided that the interaction line is either singly connected to the correlating bond or is doubly connected to a pair of bonds lying on two separate chains (see diagrams d_4, f_1, and g_2 in Figure 3). The analog of eq 4.4 for diagrams d_4 and g_2 takes a slightly more complicated form

$$C_i^{\text{random}} - C_i^{\text{diblock}} = \epsilon_{AA}\{[X_i^{(A)} + Y_i(n_A - f)]^2 - [X_i^{(A)} + Y_i(n_A - {}^1/_2)]^2\} + \epsilon_{BB}\{[X_i^{(B)} + Y_i[n_B - (1 - f)]]^2 - [X_i^{(B)} + Y_i(n_B - {}^1/_2)]^2\} + 2\epsilon_{AB}\{[X_i^{(A)} + Y_i(n_A - f)][X_i^{(B)} + Y_i[n_B - (1 - f)]] - [X_i^{(A)} + Y_i(n_A - {}^1/_2)][X_i^{(B)} + Y_i(n_B - {}^1/_2)]\} \quad (4.5)$$

with $i = d_4$ or g_2, $f = n_A/(n_A+n_B)$, and with the Y_i terms (or order $1/M$) common for the three $\epsilon_{\alpha\beta}$. Again, the difference $C_i^{\text{random}} - C_i^{\text{diblock}}$ vanishes when $f = {}^1/_2$. A related structure to that of eq 4.5 is found for diagram f_1 of Figure 3.

In addition to the energy diagrams whose monomer sequence dependence emerges in the form of $1/M$ corrections, there are more significant ones for which the monomer sequence dependent contributions are of order M^0. These diagrams describe interactions between monomer portions that are already connected to each other by a correlating bond and are called "closed loop" diagrams. Diagrams d_1, f_2, g_1, and j_3 of Figure 3 illustrate the various possible combinations of first-order closed loop interactions. The number of closed loop diagrams grows rapidly with the addition of interaction lines, but since the second-order (l=2) energy diagrams contribute much less to the high-temperature thermodynamic properties than the first-order energy diagrams, the analysis is limited here to the four first-order closed loop energy diagrams.

The contributions C_i from closed loop diagrams are again decomposed into individual terms that are either insensitive or sensitive to the monomer sequence. As with the "entropy" diagrams l and k of Figure 2, diagrams j_3 and g_1 of Figure 3 must be combined together in order to eliminate the $M \rightarrow \infty$ singularity which appears when either of these two diagrams is evaluated independently but which cancels (due to the Flory theorem[24]) upon the addition of these two diverging contributions. The values of the closed loop diagrams are summarized by

$$C_i^{\text{random}} = \epsilon_{AA}[X_i^{(AA)} + [Y_i^{(AA)} - \alpha_i Y_i^{(AB)}]f] + \epsilon_{BB}[X_i^{(BB)} + [Y_i^{(BB)} - \alpha_i Y_i^{(AB)}](1 - f)] + 2\epsilon_{AB} Y_i^{(AB)} n_A n_B/(n_A + n_B) \quad (4.6a)$$

for random copolymers and by

$$C_i^{\text{diblock}} = \epsilon_{AA}[X_i^{(AA)} + Y_i^{(AA)}] + \epsilon_{BB}[X_i^{(BB)} + Y_i^{(BB)}] + \epsilon_{AB} Y_i^{(AB)} \quad (4.6b)$$

for diblock copolymers. The subscript i in eqs 4.6a and 4.6b runs over d_1, f_2, and $j_3 + g_1$, while the coefficient α_i ranges between 0 and ${}^3/_4$. (For example, $\alpha_{d_1} = 0$, $\alpha_{f_2} = {}^1/_2$, and $\alpha_{j_3+g_1} = {}^3/_4$). Equations 4.6a and 4.6b demonstrate an essential difference between the C_i from random and diblock copolymer closed loop energy diagrams, a difference that cannot be removed simply by adjusting n_A and n_B as for many of the diagrams already discussed. This difference appears in each coefficient of the three $\{\epsilon_{\alpha\beta}\}$ for these two systems. The various coefficients come, in turn, from bond configurations involving the connecting bonds. The differences between the random and diblock copolymer melts emerge particularly from the presence of different numbers of AA, BB, and AB connecting bonds in these systems. A diblock copolymer chain contains only one AB junction bond (and hence one closed loop type interaction between A and B subunits), while a purely random copolymber generates many closed loop A−B interactions, as well as different numbers of closed loop A−A and B−B contacts than a diblock copolymer. The terms $Y_i^{(AA)}$ and $Y_i^{(BB)}$ are order of unity, in contrast to the $Y_i^{(AB)}$ contributions that are on the order of $1/M$. The monomer sequence dependence again arises here explicitly from pairs of sequential monomers, not triads as previously assumed.

Another class of diagrams contributing to the monomer sequence dependence of $\bar{F}$ is illustrated by diagram h_2 of Figure 3. This diagram contains an interaction line that is singly connected to one of three bonds that are located nonsequentially as two sets on the same chain. This combination of correlating bonds appears in the packing entropy diagram h of Figure 2 and yields a $1/M$ monomer sequence contribution to the averaged free energy $\bar{F}$. The presence of the interaction line in diagram h_2 makes this contribution much larger, i.e., of order M^0 as represented by

$$C_{h'_2}^{\text{random}} = \bar{\epsilon}_A[X_{h'_2}^{(A)} + Y_{h'_2}^{(A)}[n_A - f] + (1/2)[Z_{h'_2}^{(B)} - Z_{h'_2}^{(A)}]n_A n_B/(n_A + n_B) + 2fV_{h'_2}] + \bar{\epsilon}_B[X_{h'_2}^{(B)} + Y_{h'_2}^{(B)}[n_B - (1 - f)] + (1/2)[Z_{h'_2}^{(A)} - Z_{h'_2}^{(B)}]n_A n_B/(n_A + n_B) + 2(1 - f)V_{h'_2}] \quad (4.7)$$

and

$$C_{h'_2}^{\text{diblock}} = \bar{\epsilon}_A[X_{h'_2}^{(A)} + Y_{h'_2}^{(A)}[n_A - {}^1/_2] + (1/4)[Z_{h'_2}^{(B)} - Z_{h'_2}^{(A)}] + 2[-(1/4)n_A + (1/4)n_B + {}^1/_2]V_{h'_2}] + \bar{\epsilon}_B[X_{h'_2}^{(B)} + Y_{h'_2}^{(B)}[n_B - {}^1/_2] + (1/4)[Z_{h'_2}^{(A)} - Z_{h'_2}^{(B)}] + 2[-(1/4)n_B + (1/4)n_A + {}^1/_2]V_{h'_2}] \quad (4.8)$$

The terms $Y_{h'_2}^{(A)}$, $Y_{h'_2}^{(B)}$, $Z_{h'_2}^{(A)}$, $Z_{h'_2}^{(B)}$, and $V_{h'_2}$ of eqs 4.7 and 4.8 are of order $1/M$, and the subscript h'_2 designates the sum of diagram h_2 and the portion of diagram f_4 that is

required to be added in order to satisfy the Flory theorem[24] and to produce a meaningful physical result in the $M \rightarrow \infty$ limit. The leading order (M^0) monomer sequence dependent contributions $Z_{h'_2}^{(A)}$ and $Z_{h'_2}^{(B)}$ arise from configurations containing the connecting bonds and do not vanish when $f = {}^1/_2$. They also depend on a pair of sequential monomers on a chain.

V. Summary and Concluding Remarks

Our focus on random copolymers arises from their numerous technological and commercial applications and from the significant scientific interest in these systems. The earliest theories of random copolymer systems are based on FH theory which does not distinguish between systems of block copolymers, random copolymers, alternating copolymers, etc., with the same monomer compositions. This insensitivity of FH theory to monomer sequence and monomer structure persists in all the earliest theories, raising questions of their general validity for copolymer systems. Some attempts to rectify this inadequacy have proceeded[11,12] by introducing a set of phenomenological sequence-dependent χ parameters describing interactions between all possible triads of monomers on one chain with the triads on another. Balazs et al.[11] and Cantow and Schulz[12] reduce the number of these monomer sequence dependent χ parameters to just a few by invoking quite arbitrary assumptions.

The LCT is a natural vehicle for probing the influence of the monomer sequence distribution on the thermodynamic properties of AB copolymer systems, in part, because the LCT assigns[20] different molecular structures for the A and B monomeric species and considers different interactions between the united atom groups of the two species. These two features of the LCT have already been combined with its improved description of chain connectivity to explain the influence of local correlations upon the thermodynamics of polymer systems. Stronger disparities in the monomer structures and in their mutual interactions must inevitably lead to larger differences in the thermodynamic behavior of systems with various different sequences but with the same monomer compositions.

The main goal of the present paper is to deduce the physical nature of the leading sequence-dependent contributions to the averaged free energy of a random copolymer melt. The goal is accomplished by analyzing the contributions from the individual LCT diagrams for the free energy of random and diblock copolymer melts. Terms that differ for these two systems are identified as monomer sequence dependent. An additional benefit of the this approach lies in the possibility of extracting the particular monomer topologies and local chain conformations that directly produce the monomer sequence dependence in the averaged free energy.

Simple considerations imply that the conformations contributing to the leading sequence-dependent terms in the averaged free energy must generally involve one or more of the bonds connecting successive monomers in a chain. This is clear since different types of A−B copolymers first begin to manifest their monomer sequence through the different numbers of AA, BB, and AB connecting bonds. For instance, while a diblock copolymer chain contains only one A−B junction bond, an average random copolymer chain has many A−B bonds, but not as many as in an alternating copolymer chain, which, in turn, has no A−A and B−B connecting bonds. Bonds interior to monomers A and B may be present in the important configurations only when they appear in conjunction with the connecting bonds. The next manifestations of sequence dependence arise from triads of monomers, with the simplest configurations of this type having two connecting bonds. However, our calculations demonstrate that the leading monomer sequence contributions to the averaged free energy emerge from configurations with a pair of sequential monomers on one chains. More detailed computations are required to settle the important question concerning the nature of these leading contributions, i.e., whether they represent pair−pair or pair−monomer type interactions and whether they contain both entropic and enthalpic components.

The LCT describes the corrections to FH theory in terms of diagrams which depict successively larger clusters of submonomer units (united atom groups) that occupy single lattice sites. Each submonomer unit of the cluster is identified in a diagram by a vertex, and each bonded nearest-neighbor pair of vertices is linked by a "correlating bond", which corresponds to the actual bond in the polymer chain. Athermal limit entropic corrections to FH theory are represented by diagrams having only correlating bonds. Contributions from all these diagrams are evaluated separately and are then added together to provide the noncombinatorial athermal limit packing entropy S_{ncom}^{∞}. The computations apply strict excluded volume constraints to all submonomer units delineated in the correlating bonds of each individual diagram. All other excluded volume interactions involving the remaining united atom groups in the melt are treated[16] in a Flory−Huggins like fashion, i.e., with the neglect of all bonding-induced correlations both between the monomer portions displayed in a diagram and the rest of the system and between the monomer portions in the rest of the system.

Nearest-neighbor attractive van der Waals interactions are introduced into diagrams through the use of interaction lines connecting the pair of interacting submonomer units that lie on nearest-neighbor lattice sites. The submonomer units connected by an interaction line may either coincide with or be distinct from the units on the correlating bond(s). The latter distinct subunits are called uncorrelated units as explained below. Monomer subunits already connected by the correlating bond can interact as well, leading to what is called "closed loop" diagrams in which the interaction line connects the same pair of subunits that is attached by one of the correlating bonds. As with the athermal entropy diagrams, strict excluded volume constraints are imposed[16] on all bonded monomer groups within the cluster. The van der Waals interactions are handled[16] differently depending on whether the interacting subunits coincide or not with the subunits linked by the correlation bonds. The contributions from the interacting subunits on correlating bonds are calculated exactly (i.e., without ignoring local chain connectivity), while those arising from the uncorrelated units are again approximated in a Flory-like fashion. Diagrams with single interaction lines contribute to the system's internal energy, while diagrams with two or more interaction lines determine the temperature dependence of both the system's entropy and internal energy.

Sequence-dependent contributions to the average free energy appear both in the athermal limit entropy and in the first-order energy. The entropic terms $\bar{F}_{ij}^{(S)}$ emerge from three bond configurations in a single chain, with two bonds located in the side group of a single monomer of either species A or B and with the third bond connecting this monomer to its neighbor along the chain. The subscript *ij* in the notation $\bar{F}_{ij}^{(S)}$ emphasizes that the origin of the sequence dependence in $\bar{F}^{(S)}$ arises

from neighboring pairs *ij* of monomers on a chain. The contribution $\bar{F}_{ij}^{(S)}$ is in the form of $1/M$ corrections to the $1/z^2$ portion of the overall averaged free energy. However, this $\bar{F}_{ij}^{(S)}$ vanishes when the average numbers of A and B monomers in a single chain are equal to each other or when the monomer structures become identical.

The energetic component $\bar{F}^{(E)}$ of the sequence-dependent portion of the averaged free energy $\bar{F}$ arises from variety of different bonding configurations. The simplest example (class 1) involves a single connecting bond (AA, BB, or AB) and a single uncorrelated monomer of species A or B. The uncorrelated monomer unit must lie on a different chain than the correlating bond since we retain only terms quadratic or higher in the polymer volume fraction ϕ, i.e., terms contributing to spinodals. Various categories of these contributions have the connecting bond appearing in conjunction with additional bond(s) interior to monomers of either species A or B of the same chain. A set of three sequential bonds may contain two connecting bonds, and this pattern (class 2) provides the first manifestation of a possible sequence dependence arising from triads of monomers on a chain.

The contributions from class 1 and class 2 terms are order of $1/M$ and occur only for random copolymer melts with different averaged numbers of monomers A and B in a single chain and with different interaction energies ϵ_{AA}, ϵ_{BB}, and ϵ_{AB}. The same $1/M$ behavior is exhibited by contributions from monomer configurations which contain a connecting bond, an uncorrelated submonomer unit, and one or two bonds belonging to other chains. The leading order M^0 sequence-dependent contributions to $F^{(E)}$ emerge, however, from interactions of monomer subunits that are already linked by the connecting bond (class 3). These leading terms are independent of the molecular weight, and the sequence dependence persists for any numbers of A and B monomers in the A/B random copolymer chains. The importance of the class 3 monomer configurations is easily understood from the very different numbers of AB, AA, and BB connecting bonds in random and diblock copolymer chains with the same monomer compositions. The simplest class 3 configuration contributing to the sequence-dependent $\bar{F}^{(E)}$ beyond linear terms in ϕ involves two correlating bonds (with at least one of them as a connecting bond) lying on separate chains and with one interaction line connecting the same monomers as a connecting bond.

The leading $1/M$ sequence-dependent terms $\bar{F}_{ij}^{(S)}$ of the athermal entropy may be also written as $\bar{F}_{ij}^{(S)} = \phi^2\chi_{ij,C}^{(S)}$, where $\chi_{ij,c}^{(S)}$ is the corresponding "interaction" parameter. The subscripts *i* and *j* denote the sequential monomers on a single chain, while the symbol C designates an arbitrary pair of bonded submonomer units lying on a different chain. The number of these pairs on the other chain does not depend on the monomer sequence and always equals $M - 1$. Thus, the resulting contribution to $\chi_{ij,C}^{(S)}$ from the single bond on the second chain is unspecific with regard to the monomer sequence. Higher order contributions undoubtedly should introduce a dependence on the monomers (and sequence) in the second chain.

A similar notation applied to the sequence-dependent terms $\bar{F}^{(E)}$ of the averaged internal energy,

$$\bar{F}^{(E)} = \phi^2(\chi_{ij,C}^{(E)} + \chi_{ijk,C}^{(E)}) \tag{5.1}$$

emphasizes that $\bar{F}^{(E)}$ depends explicitly on diads and triads of monomers on one chain. The subscript C in eq 5.1 likewise represents a single correlating bond or a single uncorrelated submonomer unit that is located on a separate chain. The combinatorial factors enumerating the configurations on the separate chain are insensitive to the monomer sequence. The main difference between $\chi_{ij,C}^{(E)}$ and $\chi_{ijk,C}^{(E)}$ lies in their order in *M*. While $\chi_{ijk,C}^{(E)}$ is of order $1/M$, the contributions to $\chi_{ij,C}^{(E)}$ from "closed loop" configurations are of order M^0.

We may also apply the same analysis to the more conventional lattice model in which each monomer occupies a single lattice site. Then, all bonds in the random copolymer chain are connecting bonds. No entropic sequence-dependent contributions arise, but the presence of three different interaction energies leads to nonrandom mixing and, therefore, again to enthalpic sequence-dependent terms, as described above.

The treatment of the monomer sequence dependence of the averaged free energy $\bar{F}$ for a random copolymer melt follows naturally from the diagrammatic formalism of the LCT. No ad hoc assumptions are required concerning the particular form of χ, and no additional adjustable parameters appear beyond those already present in the theory for binary homopolymer blends. In this context, our approach is much simpler physically than the analysis of Balazs et al.[11] and of Cantow and Schulz[12] which needs several new adjustable parameters. The systematic LCT description of the monomer sequence has been possible only because the LCT considers local correlations and ascribes different molecular structures and different interactions to the chemically different monomers. Our calculations are confined to the simplest leading order diagrams that produce a sequence dependence. The same type of sequence-dependent terms appear for more complex blends such as A-*co*-B/C, A_{n_A}-*co*-B_{n_B}/$A_{n'_A}$-*co*-$B_{n'_B}$, etc., systems. Higher order diagrams evidently produce more complex monomer sequence dependent terms, such as those represented as $\chi_{ij,kl}$ or $\chi_{ijk,lmn}$, but these terms are smaller and numerically much less relevant. The LCT enables their generation without resorting to extra adjustable parameters. However, it remains to be seen how many of these sequence-dependent contributions must be retained in order to explain experimental data.

Acknowledgment. This research is supported, in part, by NSF DMR Grant No. 95-30403. We are grateful to Mary J. Jay and Ken Foreman for helpful comments on the manuscript.

Appendix A: Monomer Sequence Dependence of the Athermal Limit Packing Entropy for a Random Copolymer Melt

As mentioned in section IV, diagrams h and l of Figure 2 are the only athermal limit packing entropy diagrams that contribute to the monomer sequence dependence of the noncombinatorial entropy S_{ncom}^{∞} for a random copolymer melt. Here we provide some computational details illustrating the origin of this monomer sequence dependence and its relation to the monomer structures.

According to the general rules discussed extensively in refs 13 and 16, the contribution C_h from the diagram $D_h(b=\{1;3\},l=0)$ for a one-component polymer system may be written in the general form

$$C_h(b=\{1;3\},l=0) = \frac{2\phi^2}{z^2M^2}N_1N_3 \tag{A.1}$$

where ϕ is the volume fraction of the polymer species, *z* is the lattice coordination number, *M* designates the

single chain occupancy index, and the $\{N_i\}$ are geometrical coefficients, which represent the numbers of distinct ways for selecting a string of i consecutive bonds from a single chain. Both N_1 and N_3 as well as M depend on the monomer structures. The quantity N_1 always equals $M-1$ regardless of whether the polymer chain is a homopolymer, diblock copolymer, random copolymer, etc., but N_3 (and all the other $\{N_i\}$) vary with the monomer structures and the type of polymer chain. The coefficient N_3 for an average random copolymer chain with n_A vinyl monomers of species A and n_B vinyl monomers of species B (see top structure in Figure 1) is expressed as

$$N_3^{\text{random}} = K_3^{(A)} n_A + K_3^{(B)} n_B + I_3^{(A)}[n_A - n_A/(n_A + n_B)] + I_3^{(B)}[n_B - n_B/(n_A + n_B)] + 4n_A + 4n_B - 5 \quad \text{(A.2a)}$$

where $K_3^{(\alpha)}$ counts the number of distinct configurations of three consecutive bonds configurations within a single monomer of species α, while $I_3^{(\alpha)}$ enumerates only those three consecutive bond topologies which have two bonds in the side group of monomer α and the third consecutive bond lying on the chain backbone as the connecting bond between this monomer and one of its bonded neighbors. Hence, the coefficients $K_3^{(\alpha)}$ and $I_3^{(\alpha)}$ refer to the properties of a single monomer of species α.

A different number N_3^{diblock} of three sequential bond configurations emerges for a diblock copolymer chain with exactly n_A and n_B monomers and with the "averaged" structure for the two bottom sequences in Figure 1

$$N_3^{\text{diblock}} = K_3^{(A)} n_A + K_3^{(B)} n_B + I_3^{(A)}(n_A - {}^1/_2) + I_3^{(B)}(n_B - {}^1/_2) + 4n_A + 4n_B - 5 \quad \text{(A.2b)}$$

The factors of $^1/_2$ appear in eq A.2b from the symmetry of the averaged diblock model. If the diblock chain is instead taken to have the sequence $(A)_{n_A}-(B)_{n_B}$, the $^1/_2$ is absent in the coefficient of $I_3^{(A)}$ in eq A.2b, and a factor of unity replaces the $^1/_2$ multiplying $I_3^{(B)}$. The reversed sequence $(B)_{n_B}-(A)_{n_A}$ leads to a switch in these zero and unity coefficients, while averaging over these two sequences removes this asymmetry as indicated in eq A.2.

Substituting the expressions for N_3 from eqs A.2a and A.2b into eq A.1 produces the contributions C_h^{random} and C_h^{diblock} that can be written in compact form as

$$C_h^{\text{random}} = X_h + n_A/(n_A + n_B) Y_h^{(A)} + n_B/(n_A + n_B) Y_h^{(B)} \quad \text{(A.3a)}$$

$$C_h^{\text{diblock}} = X_h + (1/2) Y_h^{(A)} + (1/2) Y_h^{(B)} \quad \text{(A.3b)}$$

where the terms X_h and $Y_h^{(\alpha)}$ are explicitly given by

$$X_h = \frac{2\phi^2}{z^2 M^2}[M-1][K_3^{(A)} n_A + K_3^{(B)} n_B + I_3^{(A)} n_A + I_3^{(B)} n_B + 4n_A + 4n_B - 5] \quad \text{(A.4)}$$

$$Y_h^{(\alpha)} = -\frac{2\phi^2}{z^2 M^2} I_3^{(\alpha)}, \quad \alpha = \text{A, B} \quad \text{(A.5)}$$

The contribution from diagram h of Figure 2 arising from the monomer structure dependence of S_{ncom}^{∞} is represented in eqs A.3 and A.4 by the site occupancy index $M = n_A s_A + n_B s_B$ and by the coefficients $K_3^{(A)}$, $K_3^{(B)}$, $I_3^{(A)}$, and $I_3^{(B)}$.

When a similar type of analysis is applied to diagram l of Figure 2, we obtain expressions with exactly the same structure as in eqs A.3a and A.3b apart from the substitution of the subscript l + k for h since diagrams l and k must be combined together in order to satisfy the Flory theorem. The corresponding contributions, X_{l+k} and $Y_{l+k}^{(\alpha)}$, (α = A, B) are more complicated

$$Y_{l+k}^{(\alpha)} = -\frac{2\phi^2}{z^2 M^2}[I_{12}^{(\alpha)} - K_2^{(\alpha)} + J_{12}^{(\alpha)} - K_1^{(\alpha)}]$$

$$X_{l+k} = \frac{2\phi^2}{z^2 M^2}[M-1][(K_{12}^{(A)} - K_1^{(A)} K_2^{(A)}) n_A + (K_{12}^{(B)} - K_1^{(B)} K_2^{(B)}) n_B - 14(n_A + n_B - 1) + 2] - Y_{l+k}^{(A)} n_A - Y_{l+k}^{(B)} n_B$$

where $K_i^{(\alpha)}$ is the number of sequentially bonded sets of i bonds in a single monomer of species α, $K_{ij}^{(\alpha)}$ denotes the number of two nonsequentially bonded sets with i and j sequential bonds each within a single monomer of species α, while both $I_{12}^{(\alpha)}$ and $J_{12}^{(\alpha)}$ represent specific configurations of two sequential bonds and the third nonsequential bond on the same chain, as now explained. The coefficient $I_{12}^{(\alpha)}$ is the number of all distinct configurations with the single bond lying along a connecting bond and the two sequential bonds lying in the side group of a monomer of species α that is adjacent to the connecting bond. The second coefficient $J_{12}^{(\alpha)}$ counts configurations with one of the two sequential bonds as a connecting bond and with the other two bonds lying nonsequentially within the side group of a single monomer of species α.

Appendix B: Monomer Sequence Dependence of the Internal Energy for a Random Copolymer Melt

This Appendix describes some technical aspects of deriving eqs 4.4 and 4.6 and thereby illustrates the monomer sequence dependence that is generated by the presence of different interactions in a random copolymer melt. Although eqs 4.4 and 4.6 apply for whole classes of first-order energy diagrams, the derivation below is provided for the representative diagrams b_2 and d_1 of Figure 3 from two qualitatively different classes of diagrams.

Diagram b_2 is the simplest energy diagram which contributes to the monomer sequence dependence of $\bar{F}$ since the diagram contains one correlating bond and one singly connected interaction line. The contribution C_{b_2} from the diagram $D_{b_2}(b{=}1,l{=}1)$ for a one-component copolymer system (a random or diblock melt) is given by

$$C_{b_2}(b{=}1,l{=}1) = \frac{2\phi^2}{M}[\bar{\epsilon}_A[N_{AA} + (1/2)N_{AB}] + \bar{\epsilon}_B[N_{BB} + (1/2)N_{AB}]] \quad \text{(B.1)}$$

where ϕ is the volume fraction of the polymer species, M is the single chain occupancy index, and $\bar{\epsilon}_A = \epsilon_{AA} m_A + \epsilon_{AB} m_B$ and $\bar{\epsilon}_B = \epsilon_{BB} m_B + \epsilon_{AB} m_A$ are average interaction energy variables defined in terms of the energies $\epsilon_{\alpha\beta}$ and the site occupancy fractions $m_\alpha = M_\alpha/M$. These average energies appear in eq B.1 because the uncorrelated interacting submonomer unit in diagram b_2 may belong to monomers of either species A or B. The combinatorial coefficients $\{N_{\alpha\beta}\}$ in eq B.1 designate the

numbers of connecting bonds between nearest-neighbor monomer portions of species α and β in a single chain. While a diblock copolymer chain with exactly n_A monomers of species A and n_B monomers of species B has only one A−B bond, and hence $N_{AB} = 1$, an average random copolymer chain with n_A monomer of species A and n_B monomers of species B may generate many A−B bonds. Hence, the coefficients $\{N_{\alpha\beta}\}$ for these two systems must be different,

$$N_{AB}^{\text{diblock}} = 1; \quad N_{AB}^{\text{random}} = 2n_A n_B/(n_A + n_B) \quad \text{(B.2a)}$$

$$N_{\alpha\alpha}^{\text{diblock}} = K_1^{(\alpha)} n_\alpha + n_\alpha - 1; \quad N_{\alpha\alpha}^{\text{random}} = K_1^{(\alpha)} n_\alpha + n_\alpha(n_\alpha - 1)/(n_A + n_B), \quad \alpha = \text{A, B} \quad \text{(B.2b)}$$

where $K_1^{(\alpha)}$ is the number of distinct single bonds within a single monomer of species α. When the expressions in eqs B.2a and B.2b are substituted into eq B.1, the difference ΔC_{b_2} between the contributions $C_{b_2}^{\text{random}}$ and $C_{b_2}^{\text{diblock}}$ emerges as

$$\Delta C_{b_2} \equiv C_{b_2}^{\text{random}} - C_{b_2}^{\text{diblock}} = \frac{2\phi^2}{M}[\bar{\epsilon}_A[n_A/(n_A + n_B) - {}^1/_2] + \bar{\epsilon}_B[n_B/(n_A + n_B) - {}^1/_2]] \quad \text{(B.3)}$$

Setting $Y_{b_2}^{(A)} = Y_{b_2}^{(B)} \equiv -2\phi^2/M$ converts eq B.3 into eq 4.4 of sect IV.

The next diagram considered is the simplest closed loop first-order energy diagram d_1 of Figure 3. Diagram d_1 consists of two single bonds lying on separate chains and one interaction line that joins both ends of one of these two correlating bonds. The value $C_{d_1}(b=\{1;1\},l=1)$ of the cumulant diagram $D_{d_1}(b=\{1;1\},l=1)$ is given by

$$C_{d_1} = -\frac{2\phi_2}{zM^2}[M - 1][\epsilon_{AA}N_{AA} + \epsilon_{BB}N_{BB} + \epsilon_{AB}N_{AB}] \quad \text{(B.4)}$$

The appearance of the three separate interaction energies $\epsilon_{\alpha\beta}$ in eq B.4 is typical for all the closed loop first-order energy diagrams and emerges from the presence of the doubly connected interaction line that may connect bonds lying internal to monomers or on connecting bonds in all possible ways. When a similar analysis to that described for diagram b_2 is applied to diagram d_1, we obtain

$$C_{d_1}^{\text{random}} = -\frac{2\phi^2}{zM^2}[M - 1][[\epsilon_{AA}[K_1^{(A)}n_A + n_A(n_A - 1)/(n_A + n_B) + \epsilon_{BB}[K_1^{(B)}n_B + n_B(n_B - 1)/(n_A + n_B)] + 2\epsilon_{AB}n_A n_B/(n_A + n_B)] \quad \text{(B.5)}$$

$$C_{d_1}^{\text{diblock}} = -\frac{2\phi^2}{zM^2}[M - 1][\epsilon_{AA}(K_1^{(A)}n_A + n_A - 1) + \epsilon_{BB}(K_1^{(B)}n_B + n_B - 1) + \epsilon_{AB}] \quad \text{(B.6)}$$

Introducing the new variables

$$X_{d_1}^{(\alpha\alpha)} = -\frac{2\phi^2}{zM^2}[M - 1]K_1^{(\alpha\alpha)}n_\alpha, \quad \alpha = \text{A, B}$$

$$Y_{d_1}^{(\alpha\alpha)} = -\frac{2\phi^2}{zM^2}[M - 1][n_\alpha - 1], \quad \alpha = \text{A, B}$$

$$Y_{d_1}^{(AB)} = -\frac{2\phi^2}{zM^2}[M - 1]$$

and $f = n_A/(n_A + n_B)$ converts these equations into eqs 4.6a and 4.6b with $\alpha_{d_1} = 0$.

References and Notes

(1) *Encyclopedia of Polymer Science and Engineering*; Kroschwitz, J. I., Ed.; Wiley: New York, 1990.
(2) Roe, R. J.; Zim, W. C. *Macromolecules* **1980**, *13*, 1221. Paul, D. R.; Barlow, J. W. *Polymer* **1984**, *25*, 487.
(3) Kambur, R. P.; Bendler, J. T.; Bopp, R. C. *Macromolecules* **1983**, *16*, 753.
(4) ten Brinke, G.; Karasz, F. E.; MacKnight, W. J. *Macromolecules* **1983**, *16*, 1827.
(5) Roe, R. J.; Rigby, D. *Adv. Polym. Sci.* **1987**, *82*, 103. Huh, W.; Karasz, F. E. *Macromolecules* **1992**, *25*, 1057.
(6) Gersappe, D.; Balazs, A. C. *Phys. Rev. E* **1995**, *52*, 5061. Milner, S. T.; Fredrickson, G. H. *Macromolecules* **1995**, *28*, 7953.
(7) Winley, K. I.; Berba, M. L.; Galvin, M. E. *Macromolecules* **1996**, *29*, 2868.
(8) Lohse, D. J.; Graessley, W. W., unpublished results.
(9) Jinnai, H.; Hasegawa, H.; Hashimoto, T.; Han, C. C. *Macromolecules* **1992**, *25*, 6078.
(10) Chai, Z.; Sun, R.; Karasz, F. E. *Macromolecules* **1992**, *25*, 6113.
(11) Balazs, A. C.; Sanchez, I. R.; Epstein, I. R.; Karasz, F. E.; MacKnight, W. J. *Macromolecules* **1985**, *18*, 2188.
(12) Cantow, H. J.; Schulz, O. *Polym. Bull.* **1986**, *15*, 449.
(13) Dudowicz, J.; Freed, K. F. *J. Chem. Phys.* **1994**, *100*, 4653.
(14) Freed, K. F.; Dudowicz, J. *J. Chem. Phys.* **1992**, *97*, 2105. Dudowicz, J.; Freed, K. F. *Macromolecules* **1993**, *26*, 213.
(15) Dudowicz, J.; Freed, K. F.; Madden, W. G. *Macromolecules* **1990**, *23*, 4803.
(16) Dudowicz, J.; Freed, K. F. *Macromolecules* **1991**, *24*, 5076.
(17) Dudowicz, J.; Freed, M. S.; Freed, K. F. *Macromolecules* **1991**, *24*, 5096.
(18) Dudowicz, J.; Freed, K. F.; Douglas, J. F. *Macromolecules* **1995**, *28*, 2276.
(19) Freed, K. F.; Dudowicz, J. *Trends Polym. Sci.* **1995**, *3*, 248.
(20) Freed, K. F.; Dudowicz, J., to be published.
(21) Dudowicz, J.; Freed, K. F. *Macromolecules* **1991**, *24*, 5112.
(22) Madden, W. G. *J. Chem. Phys.* **1990**, *92*, 2055.
(23) The missing letters refer to the diagrams, linear in ϕ, which may be found in ref 16.
(24) Flory, P. J. *Principles of Polymer Chemistry*; Cornell University Press: Ithaca, NY, 1953.

MA960587V